Scanning tunneling microscopy study of self-organized Au atomic chain growth on Ge(001)

J. Wang,[1] M. Li,[2] and E. I. Altman[2]
[1]*Department of Physics, Yale University, New Haven, Connecticut 06520, USA*
[2]*Department of Chemical Engineering, Yale University, New Haven, Connecticut 06520, USA*
(Received 10 May 2004; revised manuscript received 15 July 2004; published 23 December 2004)

Gold deposition onto Ge(001) at 675 K led to self-organized atomic chains in (4×2) and c(8×2) surface reconstructions. The chains were separated by 1.6 nm and ran up to several hundred nanometers long. The Au-induced domains showed alternating white and gray chains in STM images that could be explained by Au-Au and mixed Au-Ge dimer rows, respectively. The chains showed a zigzag pattern attributed to dimer buckling. Bias-dependent STM imaging suggested that the Au chains were metallic nanowires. The chains, however, were not defect-free and contained missing dimer vacancies. The Ge terraces adjacent to the Au nanowire domains contained a high density of $(1+2+1)$ dimer vacancy defects that tended to run along [100] and [310] directions. The above results show strong similarities with those obtained for Pt on Ge(001) but are very different from those for Ag, which only weakly interacted with Ge(001), and thus support models suggesting stronger bonding of low-coordinated atoms of the 5*d* metals compared to the corresponding 4*d* metals.

DOI: 10.1103/PhysRevB.70.233312 PACS number(s): 68.35.Ct, 68.37.Ef

Metal nanowires have attracted interest because their electronic transport properties are important for advances in fundamental physics and continued progress in electronic device miniaturization. It has been pointed out that the 5*d* metals Ir, Pt, and Au tend to form surface reconstructions containing atomic chains on their own low-index surfaces.[1,2] Recent experiments reporting the formation of one-atom-thick metallic Pt chains on Ge(001) suggest that this property can be exploited to create nanowires.[3] Previous work on the initial growth of Au on Si(001) showed chain-like surface reconstructions supporting this idea.[4–7] On the other hand, Au is chemically more similar to Ag, as borne out by the bulk-phase diagrams that show that Au and Ag are essentially immiscible in Ge while Pt forms a series of well-defined intermetallic phases.[8] Our previous study of Ag growth on Ge(001) showed that Ag favored three-dimensional cluster formation, although metastable two-dimensional Ag-Ge surface alloys could be formed by depositing Ag in a narrow temperature window.[9] Thus, comparing Au with Ag and Pt growth on Ge(001) offers the opportunity to test the growing consensus that there is a stronger bonding of low-coordinated atoms of the 5*d* metals compared to the corresponding 4*d* metals that results from *sd* competition caused by relativistic effects in the electronic structure.[2,10,11] In this paper, it will be shown that Au does in fact behave similarly to Pt on Ge(001), forming conductive atomic chains in (4×2) and c(8×2) reconstructions that can be explained by Au-Au and Au-Ge dimers.

The experiments were conducted using an ultrahigh-vacuum (UHV) system equipped with a sputter-ion gun, resistively heated evaporation sources, an electron spectrometer for Auger electron spectroscopy (AES), low energy electron diffraction (LEED) optics, and a custom-designed variable temperature scanning tunneling microscope.[12] The Ge(001) samples were cut from a nominally undoped Ge wafer with a resistivity of 5.5 Ω-cm obtained from Atomergic Chemetals Corp. The temperature was measured using a K-type thermocouple housed in a thin Ta tube pressed against the front face of the sample. The Ge(001) substrate was prepared by cycles of 500 eV Ar^+ sputtering and annealing at 940 K until no contaminants were detected by AES. A 10–20-nm-thick Ge buffer layer was then deposited at 620 K and annealed to 940 K to produce large flat terraces with very few surface defects and a sharp (2×1) LEED pattern.[13] Gold and Ge were deposited by resistively heating tungsten baskets filled with the materials. The deposition rates were measured with a quartz crystal microbalance calibrated using scanning tunneling microscopy (STM). The coverages reported refer to the amount of Au deposited; because Au can move beneath the surface under the experimental conditions, it is difficult to determine the Au coverage in the ordered structures seen. The STM images were recorded at room temperature.

The clean Ge(001) surface showed a (2×1) reconstruction with large flat terraces composed of dimer rows rotated 90° on alternating terraces. STM images of the surface revealed few defects and the bands of buckled and nonbuckled dimers favored on Ge(001).[14] After deposition of 0.5 ML of Au at 675 K, a (4×2) LEED pattern was seen. The STM images of such surfaces are shown in Fig. 1. In the large-scale image, Fig. 1(a), a few domains of Au-induced chains can be seen together with the dimerized Ge(001) surface. The Au-induced chains can be up to several hundred nanometers long. Antiphase domain boundaries (APBs) both parallel and perpendicular to the chains can be seen, as indicated by the arrows. The smaller scale images in Figs. 1(b) and 1(c) show that the alternating white and gray rows that make up the (4×2) reconstruction existed adjacent to the original Ge dimer rows with the chains paralleling the neighboring Ge dimer rows. The chains appear higher than the neighboring Ge dimer rows in the STM images; however, this cannot be clearly attributed to a topographic height difference between Au and Ge, since Ge and Au have very different electronic structures. As shown in the height profile [Fig. 1(d)] across the chains and the adjacent Ge dimer rows, the brighter chains are about 0.13 nm higher than the Ge dimer rows in the same layer, while the gray chains are around 0.03 nm higher than Ge. Also note the parallel APB at the bottom right of Fig. 1(c), which demonstrates that the appearance of the gray chains is not due to a tip artifact. Also,

 ©2004 The American Physical Society

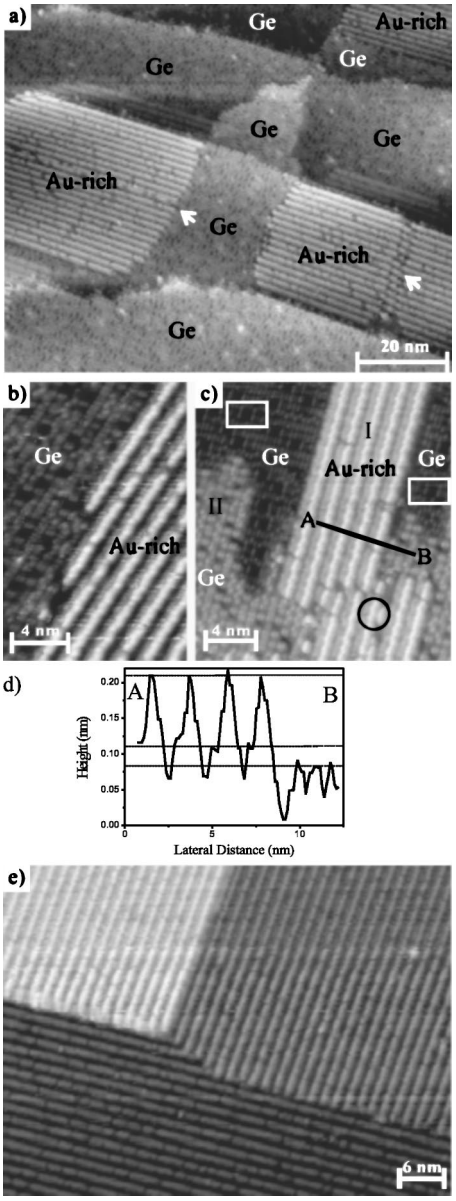

FIG. 1. Large (a) and small (b) scale STM images obtained after depositing 0.5 ML Au on Ge(001) at a rate of 0.6 ML/min at 675 K. (c) STM image of 0.5 ML Au deposited on Ge(001) at 0.7 ML/min at 575 K. (d) Line profile obtained through AB in (c). (e) STM image of 1.5 ML Au deposited on Ge(001) at 675 K. Sample biases were (a) −1.5 V; (b) −0.8 V; (c) −1.5 V; and (e) −1.5 V.

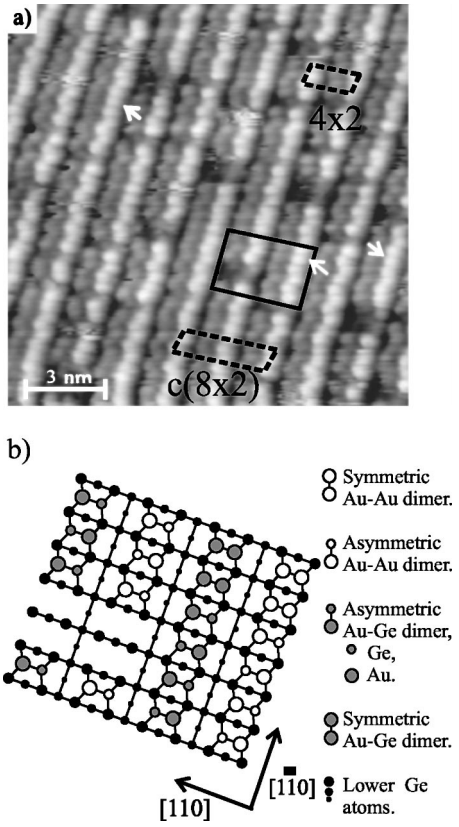

FIG. 2. (a) High-resolution STM image of 1.5 ML of Au deposited on Ge(001) at a rate of 0.6 ML/min at 675 K; the sample bias was −0.7 V. (b) Ball and stick model for the region surrounded by the solid parallelogram in (a).

the substrate vacancies highlighted by the boxes show no evidence of shadowing due to a double tip. The chains could be imaged well down to 0.2 V sample bias while the neighboring Ge patches could not, suggesting that the chains were metallic and at a minimum, indicating that they have a smaller bandgap than the reconstructed Ge surface.

As shown in Figs. 1(c) and 2(a), both the white and gray chains in the reconstructed domains show a zigzag pattern similar to that attributed to dimer buckling on the clean Ge(001) surface, though in Fig. 1(c) it is clear that the height variation along the Au-induced chains is smaller than that in buckled Ge dimer rows; the typical height variations obtained from Fig. 1(c) are 0.035 nm for Au chains and 0.06 nm for Ge dimer rows. The alternating zigzag pattern in the neighboring chains creates a $c(8\times2)$ unit cell as highlighted by the dashed parallelogram at the bottom of Fig. 2(a). A (4×2) unit cell consistent with the LEED results, highlighted at the upper right of Fig. 2(a), is obtained if we consider only the gross positions of the atoms and not the small asymmetry of the chains.

From the high-resolution filled state STM image of the Au-induced structure shown in Fig. 2(a), the structural model of the chains based on Au-Au and Au-Ge dimer rows in Fig. 2(b) was constructed. The model shows the region in Fig. 2(a) bounded by the solid parallelogram, including the vacancies. In the model, white circles represent Au atoms in epitaxial Au-Au dimers, and the large and small gray circles represent Au and Ge atoms, respectively, in epitaxial Au -Ge dimers. The Au-Au dimer rows are assigned to the white chains in the STM images and the Au-Ge dimers to the gray chains; the apparent height differences in the images can be attributed to a higher electron density near the Fermi level for Au atoms compared to Ge atoms. As shown in Fig. 1(c), which was obtained at 575 K so the domains are smaller than at 675 K,[15] both the white and gray Au chains in the centered right part of the image (marked region "I") appear higher than the neighboring Ge dimer rows in the left (marked "II"). The bright chains look about 0.13 nm higher than the Ge dimer rows, while the gray chains are about

0.03 nm higher than the Ge. However, they were all considered to be at the same level, with the height difference attributed to Au incorporation increasing the state density near the Fermi level. In the model, the zigzag pattern of the white chains is associated with buckling of the Au dimers, while the pattern in the gray chains may be due to either buckling or electronic differences between the Au and Ge atoms in the mixed dimers. Compared to the clean Ge substrate where roughly half of the dimers appear buckled in a $c(4\times2)$ pattern,[14] nearly all of the Au-Au dimers were buckled. On Ge and Si(001) buckled dimers are generally considered the lowest energy state with the unbuckled appearance observed in room temperature STM images attributed to a rapid flipping between the two equivalent buckled configurations.[16] This suggests a higher barrier to flip Au-Au dimers than Si-Si dimers and Ge-Ge dimers in nonbuckled (2×1) domains. Alternatively, differences in interactions between Au-Au dimers and Au-Ge dimers in neighboring rows depending on whether a Au or Ge atom is closest to the dimer may lock the buckling; however, chains with the higher Au atom in the Au-Au dimer adjacent to both the higher and lower spot in the gray chains were observed. The buckling of the Au chains can also be caused by the vacancies in the Au-induced domains. As can be seen from the atomic scale STM images, both the Au-induced domains and the Ge substrate showed more vacancies than clean Ge(001). The tension difference between the two sides of the dimers neighboring the defects could freeze the buckling of the Au chains. Some unbuckled dimers could be seen, as highlighted by the arrows in Fig. 2(a), and these all avoided the vacancies supporting the above argument.

Many experimental and theoretical studies of epitaxial metal growth on Ge and Si(001) substrates showed that the metal atoms tended to form dimers on the surface, such as Ag on Ge(001),[9,17,18] Al on Si and Ge(001),[19,20] Pt on Ge(001),[3] etc. Our model of Au on Ge(001) is constructed from the same elements proposed to explain Pt-induced nanowires on Ge(001).[3] For Pt, however, it was suggested that the Pt-Pt dimers were one level higher than the mixed Pt-Ge dimers, and thus perpendicular to the Pt-Ge dimers. This model cannot explain the zigzag appearance of the white chains, and thus for Au we favor the model described above with the Au-Au dimers on the same level and parallel to the mixed dimers.

The surface area covered by Au-induced chains increased as more Au was deposited. As shown in the image in Fig. 1(e), where 1.5 ML of Au was deposited at 675 K, the surface was fully covered with well-ordered chains running along the [110] and $[1\bar{1}0]$ directions. When the annealing temperature was increased towards the Ge melting point, no new structures were observed and eventually the chains disappeared and Auger indicated loss of Au from the surface. The bulk-phase diagram indicates that ~50 ML of Au can be accommodated within our Ge samples at high temperatures, and so the disappearance of the Au can be attributed to bulk migration.[8]

The images of the Ge dimer rows after Au deposition show a high defect density; a closer look at these defects is provided in Fig. 3, where the images were obtained after depositing 0.1 ML Au at 675 K. As seen in Figs. 3(a)–3(c), there were no Au-induced chains on the surface, indicating that all of the Au went beneath the surface. The Ge substrate became vacancy-rich in order to relieve the stress caused by Au incorporation. The dimer vacancies (DVs) were not ordered over a long range as in the case of Ni- or Ag-induced vacancy lines that run perpendicular to the dimer rows on Si(001).[21–24] The Au-induced vacancies, however, were inclined to line up along the [100] and [310] directions over short ranges, as shown in Fig. 3(c). The alignment of dimer vacancy lines along the [310] direction was similar to that seen by Gurlu *et al.*[3] after Pt nanowire formation on Ge(001).

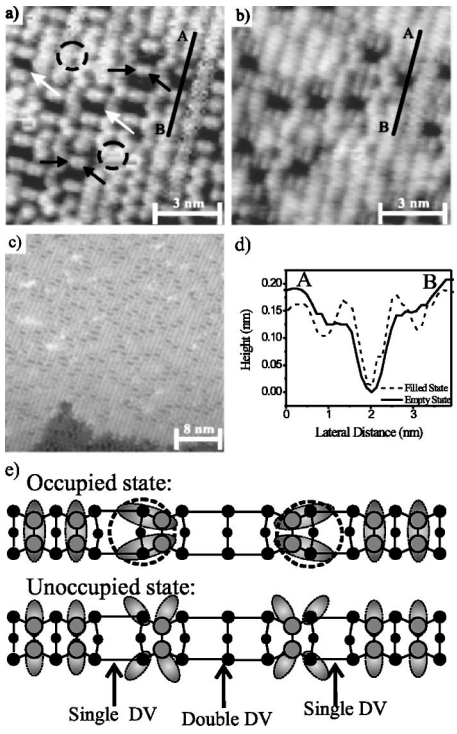

FIG. 3. Filled (a) and empty (b) state, and large-scale filled state (c) STM images recorded after depositing 0.1 ML Au onto Ge(001) at 675 K and a rate of 0.6 ML/min, sample biases were (a) −1 V; (b) 1 V; (c) −1 V. (d) Line profiles through a (1+2+1) dimer vacancy taken from filled and empty state images. (e) Ball and stick model of the (1+2+1) dimer vacancy; the black balls represent the subsurface atoms, the gray balls the surface dimers, and occupied and unoccupied electronic state densities are indicated by the ellipses.

The higher resolution image in Fig. 3(a) illustrates the types of vacancies present after Au deposition. Unlike clean Ge(001), where single and double DVs along with lower coverages of defects with two dimers missing on adjacent rows as well as the (2+1) DV (a single DV followed by a normal dimer and then a double DV) are present,[25–27] the image in Fig. 3(a) is dominated by (1+2+1) DVs, as highlighted by the white arrows, and a small amount of (2+1) DVs. The (1+2+1) DVs consisted of double DVs in the middle with two single DVs on each side along the dimer row.

A closer look at Fig. 3(a) shows many spots where the dimers appear brighter, or higher, than normal, as illustrated

by the dashed circles. Comparing the filled state image [Fig. 3(a)] with the empty state image [Fig. 3(b)] shows that this difference is more distinct in filled state images. These features were attributed to substitutional Au-Ge dimers or Au atoms beneath the outermost layer. This supports our structural model by illustrating Au incorporation into the Ge and by showing that this substitution increases the apparent height of the dimers.

Interestingly, the isolated dimers between the single and double dimer vacancies in the $(1+2+1)$ and $(1+2)$ DVs appear split in STM images, allowing the individual atoms in the dimers to be resolved. As illustrated by comparing Figs. 3(a) and 3(b), this splitting was much more dramatic in unoccupied state images at low biases. Instead of the small splitting of the dimer in the filled state image as indicated by the black arrows in Fig. 3(a), the two atoms in the isolated dimer appear significantly separate and elongated toward the neighboring single DV in Fig. 3(b). Similar split-off dimer defects were seen by Schofield *et al.* on metal-contaminated Si(001) surfaces.[28] The difference was that the Si(001) surface was dominated by $(2+1)$ DVs, while $(1+2+1)$ DVs prevailed on the Au-Ge(001) surface. The comparison between line profiles drawn across the $(1+2+1)$ DVs in Fig. 3(d) readily show the morphology and electronic differences between the filled and empty state images.

Based on the dual bias STM images and the split-off dimer model proposed by Schofield[28] and Qin,[29] the structural model of the Au-induced $(1+2+1)$ DVs shown in Fig. 3(e) is proposed. As noted by Schofield *et al.*,[28] the distance between the split-off dimer and the atoms in the single vacancy trough allows a tetramer to form. If the π bonds between the split-off dimer and trough atoms are closer to the Fermi level than the normal dimer π bond, then at low negative sample biases the tunnel current will be dominated by the electron density between the split-off dimer and trough atoms, allowing the individual atoms in the split-off dimer to be resolved;[28] the ellipses in Fig. 3(e) highlight the locations of these π bonds. This suggests that the tetramer must have unoccupied antibonding π^* levels localized as pictured in Fig. 3(e). While the antibonding levels in normal nonbuckled dimers also allow individual atoms to be resolved in empty state images, the π^* levels of the tetramer lead to a much more obvious corrugation between the atoms of the split-off dimer as shown in Fig. 3(b).

In summary, Au growth on Ge(001) at 675 K leads to (4×2) and $c(8\times2)$ reconstructions. In STM images the reconstructions appear as alternating high and low zigzag chains. The chains could be imaged at high resolution down to low biases, suggesting that they are metallic nanowires. The higher chains were attributed to rows of Au-Au buckled dimers and the lower chains to mixed Au-Ge dimers. At lower Au coverages, (2×1) reconstructed Ge with a high density of $(1+2+1)$ dimer vacancy defects was observed adjacent to the chains. These vacancies tended to align along the [100] and [310] directions but did not order over a long range. The STM images suggested that the isolated dimer bonded with the neighboring second-layer atoms to form a tetramer. In general, Au was found to behave very similarly to Pt on Ge(001) where growth of conductive chains has been observed,[3] but very differently from Ag on Ge(001) where large three-dimensional clusters are favored.[9] These results are consistent with the 5*d* metals favoring one-dimensional chain formation on surfaces; to further test this hypothesis we are currently studying Pd growth on Ge(001).

The authors thank W. Gao for his help. This project was supported by National Science Foundation through Grant Number CTS-9733416.

[1] A. I. Yanson, G. R. Bollinger, H. E. van den Brom, N. Agrait, and J. M. Ruitenbeek, Nature (London) **395**, 783 (1998).
[2] R. H. M. Smit, C. Untiedt, A. I. Yanson, and J. M. Ruitenbeek, Phys. Rev. Lett. **87**, 266102 (2001).
[3] O. Gurlu, O. A. O. Adam, H. J. W. Zandvliet, and B. Poelsema, Appl. Phys. Lett. **83**, 4610 (2003).
[4] M. Kageshima, Y. Torii, Y. Tano, O. Takeuchi, and A. Kawazu, Surf. Sci. **472**, 51 (2001).
[5] R. Hild, F.-J. Meyer Zu Heringdorf, P. Zahl, and M. Horn-von Hoegen, Surf. Sci. **454–456**, 851 (2000).
[6] T. Shimakura, H. Minoda, Y. Tanishiro, and K. Yagi, Surf. Sci. **407**, L657 (1998).
[7] X. F. Lin, K. J. Wan, J. C. Glueckstein, and J. Nogami, Phys. Rev. B **47**, 3671 (1993).
[8] T. B. Massalski and H. Okamoto, *Binary Alloy Phase Diagrams* (ASM, Cleveland, 1990).
[9] L. H. Chan and E. I. Altman, Phys. Rev. B **66**, 155339 (2002).
[10] N. Takeuchi, C. T. Chan, and K. M. Ho, Phys. Rev. Lett. **63**, 1273 (1989).
[11] P. Pyykkö, Chem. Rev. (Washington, D.C.) **88**, 563 (1988).
[12] C. Y. Nakakura, V. M. Phanse, G. Zheng, G. Bannon, E. I. Altman, and K. P. Lee, Rev. Sci. Instrum. **69**, 3251 (1998).
[13] L. H. Chan, E. I. Altman, and Y. Liang, J. Vac. Sci. Technol. A **19**, 976 (2001).
[14] H. J. W. Zandvliet, B. S. Swartzentruber, W. Wulfhekel, B. Hattink, and B. Poelsema, Phys. Rev. B **57**, R6803 (1998).
[15] J. Wang, M. Li, and E. I. Altman (unpublished).
[16] S. D. Kevan, Phys. Rev. B **32**, 2344 (1985).
[17] K. Seino and A. Ishii, Surf. Sci. **493**, 420 (2001).
[18] K. Seino and A. Ishii, Surf. Sci. **467**, 177 (2000).
[19] G. Brocks and P. J. Kelly, Phys. Rev. Lett. **70**, 2786 (1993).
[20] N. Takeuchi, Phys. Rev. B **61**, 9925 (2000).
[21] H. J. W. Zandvliet, Surf. Sci. **377–379**, 1 (1997).
[22] H. J. W. Zandvliet, H. K. Louwsma, P. E. Hegeman, and B. Poelsema, Phys. Rev. Lett. **75**, 3890 (1995).
[23] V. A. Ukraintsev and J. T. Yates, Surf. Sci. **346**, 31 (1996).
[24] C. S. Chang, Y. M. Huang, C. C. Chen, and T. T. Tsong, Surf. Sci. Lett. **367**, L8 (1996).
[25] H. J. W. Zandvliet, Phys. Rep. **388**, 1 (2003).
[26] W. S. Yang, X. D. Wang, K. Cho, J. Kishimoto, S. Fukatsu, T. Hshizume, and T. Sakurai, Phys. Rev. B **50**, 2406 (1994).
[27] M. Li and E. I. Altman, Phys. Rev. B **66**, 115313 (2002).
[28] S. R. Schofield, N. J. Curson, J. L. O'Brien, M. Y. Simmon, R. G. Clark, N. A. Marks, H. F. Wilson, G. W. Brown, and M. E. Hawley, Phys. Rev. B **69**, 085312 (2004).
[29] X. R. Qin and M. G. Lagally, Phys. Rev. B **59**, 7293 (1999).